GeoHealth

RESEARCH ARTICLE
10.1002/2017GH000125

Special Section:
Science and Exploration of the Moon, Near-Earth Asteroids, and the Moons of Mars

Assessing Toxicity and Nuclear and Mitochondrial DNA Damage Caused by Exposure of Mammalian Cells to Lunar Regolith Simulants

Rachel Caston[1,2], Katie Luc[1], Donald Hendrix[3], Joel A. Hurowitz[3], and Bruce Demple[1,2]

[1]Department of Pharmacological Sciences, Stony Brook University School of Medicine, Stony Brook, NY, USA, [2]Program in Genetics, Stony Brook University, Stony Brook, NY, USA, [3]Department of Geosciences, Stony Brook University, Stony Brook, NY, USA

Abstract Previous missions to the lunar surface implicated potential dangers of lunar soil. In future explorations, astronauts may spend weeks or months on the Moon, increasing the risk of inhaling lunar dust. In an effort to understand the biological impact of lunar regolith, cell cultures derived from lung or neuronal cells were challenged with lunar soil simulants to assess cell survival and genotoxicity. Lunar soil simulants were capable of causing cell death and DNA damage in neuronal and lung cell lines, and freshly crushed lunar soil simulants were more effective at causing cell death and DNA damage than were simulants as received from the supplier. The ability of the simulants to generate reactive oxygen species in aqueous suspensions was not correlated with their cytotoxic or genotoxic affects. Furthermore, the cytotoxicity was not correlated with the accumulation of detectable DNA lesions. These results determine that lunar soil simulants are, with variable activity, cytotoxic and genotoxic to both neuronal and lung-derived cells in culture.

Plain Language Summary Lunar dust adhering to their suits caused mild respiratory issues for Apollo astronauts returning from the Moon. Chronic or long-term effects of such dust exposure could be a problem for future missions. We assessed the cellular effects of exposure to terrestrial materials produced to mimic some aspects of lunar dust (simulants). We found significant cell toxicity in neuronal and lung cell lines in culture, as well as DNA damage associated with the exposure. Unexpectedly, these effects did not reflect the ability of the simulants to generate free radicals.

Key Points:
- Lunar soil may pose a health risk when inhaled by astronauts
- Lunar soil simulants have cytotoxic and genotoxic effects on neuronal and lung epithelial cells
- Cytotoxicity of the soils was not correlated with the DNA damage they caused in neuronal and lung cells

Correspondence to:
B. Demple,
bruce.demple@stonybrook.edu

Citation:
Caston, R., Luc, K., Hendrix, D., Hurowitz, J. A., & Demple, B. (2018). Assessing toxicity and nuclear and mitochondrial DNA damage caused by exposure of mammalian cells to lunar regolith simulants. *GeoHealth*, *2*, 139–148. https://doi.org/10.1002/2017GH000125

Received 11 DEC 2017
Accepted 3 APR 2018
Accepted article online 12 APR 2018
Published online 26 APR 2018

This article was corrected on 15 JUL 2019. The online version of this article has been modified to include a Conflict of Interest statement.

©2018. The Authors.
This is an open access article under the terms of the Creative Commons Attribution-NonCommercial-NoDerivs License, which permits use and distribution in any medium, provided the original work is properly cited, the use is non-commercial and no modifications or adaptations are made.

1. Introduction

One aspect of the lunar environment that warrants more study in preparation for human exploration is the lunar regolith or soil. Lunar soil is affected by a combination of processes that include micrometeorite impacts and the resulting agglutination, as well as exposure to the solar wind (Heiken et al., 1992). There are important differences between the lunar and terrestrial environments that affect the surface material. The Moon has no liquid component in the soil, so water-containing minerals, such as clay or mica, are not present (Heiken et al., 1992). The lack of lunar atmosphere also allows the Moon's surface to be perpetually bombarded by solar wind. The constant chemical reduction that results from this exposure causes the lunar soil to become electrostatically charged. This charge can be so strong that the soil particles actually levitate above the lunar surface (Colwell et al., 2007; Stubbs et al., 2005).

When astronauts visited the Moon during the Apollo missions, the electrostatically charged lunar soil clung to their spacesuits, such that lunar dust was carried into the living environment by astronauts who had been exploring the lunar surface (Gaier, 2007). Astronaut Harrison Schmitt described his reaction to lunar dust as "lunar hay fever," including sneezing, watering eyes, and sore throat (Wagner, 2006). Lunar dust in the lunar exploration module represents a potential biological hazard to astronauts, with particles of 5–10 μm capable of accumulating in the central airways and smaller particles, 0.5–5 μm, infiltrating the alveoli (Jabbal et al., 2017; Mckay et al., 2015). A study in rats revealed that exposure to lunar soil led to a concentration-dependent increase in lung inflammation and cytotoxicity over the course of 13 weeks (Lam et al., 2013). Additionally, there is evidence from rats that the smaller particles (≤0.1 μm) can be transported through the olfactory bulb into the brain (Oberdörster et al., 2004). However, it is not known how deep into human brains the inhaled lunar dust might infiltrate (Oberdörster et al., 2005).

Table 1
Characterization of Lunar Soil Simulants

Particulate name	Purpose or emulated location	Description
JSC-1A	Low-titanium mare	Volcanic ash from Arizona that resembles lunar maria (Ray et al., 2010)
JSC-1A agglutinated	Low-titanium mare	Treated to form glassy agglutinates (Kaur et al., 2016)
NU-LHT-2M	Highland	Replicate of lunar highland basalts (Kaur et al., 2016)
NU-LHT-2M agglutinated	Highland	Treated to form glassy agglutinates (Kaur et al., 2016)
CSM-CLF	Geotechnical	Developed from Colorado lava (Kaur et al., 2016)
Quartz	Control material	Little found on Moon; known to be cytotoxic (van Berlo et al., 2010)
Anatase (TiO_2)	Control material	Non-chemically reactive particulate (Wang et al., 2013)

Note. CSM-CLF = Colorado School of Mines - Colorado Lava (Fine).

From terrestrial studies, we understand some of the risks of breathing toxic dust. The most relevant situations occur following occupational or environmental exposure. For example, people who were exposed to volcanic ash after the eruption of Mt. St. Helens in 1980 suffered acute effects including bronchitis, wheezing, and eye irritation (Baxter et al., 1983). Those with chronic lung diseases such as asthma and emphysema were disproportionately affected (Baxter et al., 1983). A study involving the lungs of rats exposed to ashes from Arizona lava fields showed that they exhibited chronic inflammation, septal thickening, and fibrosis (Lam et al., 2002). Furthermore, workers in the mining industry are repeatedly exposed to dust from recently uncovered mineral deposits. A common outcome of this exposure is silicosis, a disease that develops from long-term exposure to crystalline silica (Rimal et al., 2005). Silicosis is a potentially fatal disease, caused by silica dust particles embedded in the alveolar sacs, resulting in shortness of breath with lung irritation and in progressive fibrosis (Rimal et al., 2005).

There is also an accumulating body of evidence on the detrimental effects of particulate matter in the brain. However, due to the inaccessibility of the brain, concrete conclusions about these effects can be difficult to obtain. General inflammation is one result, as seen in the brains of mice exposed to airborne particles, which developed neuronal inflammation, including the increased expression of the inflammatory cytokines IL-1α, TNFα, and NFκB (Campbell et al., 2005).

DNA damage resulting from dust exposure has been less well studied but is an aspect of possible long-term significance to human health. DNA damage can be both short-term and long-term problems, and it can affect both the nuclear and the mitochondrial genome. Mutations in nuclear DNA may lead to cell death or cancer, and these endpoints are not mutually exclusive (Roos & Kaina, 2013; Roos et al., 2016), because dying cells can signal to neighboring cells to promote cell division (Labi & Erlacher, 2015). Failure to repair the mitochondrial DNA is associated with neurodegenerative disorders (Cha et al., 2015). In an animal study, rats exposed to particles isolated from air pollution developed nuclear DNA mutations in their sperm (Yauk et al., 2008). For the human A549 lung cell line, treatment with various particulate materials caused DNA strand breaks and activated caspase-9, an enzyme released from mitochondria in a process of cell death (Upadhyay et al., 2003).

Due to the scarcity of lunar soil available for research, lunar soil simulants are used as a substitute (Colwell et al., 2007). The simulants are designed to mimic various aspects of lunar soil. This project uses five lunar soil simulants and two control particulate materials (Table 1). The simulants in this set were generated to mimic different types of lunar soil with distinctive compositions. Chemically reactive simulants are categorized here as those that generate reactive oxygen species (ROS). Among other mechanisms, ROS may be formed by metals exposed at surface defects in the soil particles that interact with oxygen when exposed to aqueous solutions (Turci et al., 2015). However, even some simulants selected for their physical characteristics may indirectly generate ROS in cells by triggering an inflammatory response upon contact with the cells (Sena & Chandel, 2012).

JSC-1A and the agglutinated form of JSC-1A were designed to simulate different physical and chemical aspects of regolith from the lunar mare (Ray et al., 2010). NU-LHT-2M and its agglutinated form are chemical replicates of regolith from the lunar highlands (Kaur et al., 2016). CSM-CLF is a chemically reactive soil intended to mirror the ability of lunar soil to generate ROS (Kaur et al., 2016). Quartz, a mineral, is included because its dust is known to cause silicosis (Bhagia, 2012). Compared to the lunar soil simulants, quartz does not generate high concentrations of ROS in solution (Hurowitz et al., 2007). Anatase also produces low ROS concentration in solution and serves as a control for the physical response of the cells to particulate

matter. Additionally, nanoparticle-sized anatase had lower pulmonary toxicity in rats than did quartz particles (Warheit et al., 2007).

The experiments were performed using two cell lines. The Cath.-a-differentiated (CAD) cells were isolated from a mouse neuroblastoma (Qi et al., 1997). CAD cells can be cultured for active proliferation or induced to differentiate in culture by serum starvation (Qi et al., 1997). These cells allow for genetically identical proliferating progenitors and terminally differentiated neurons to be compared directly. The A549 cell line was developed from a human lung carcinoma. A549 cells were used to represent lung exposure.

We present data showing that exposure to lunar soil simulants is cytotoxic and DNA damaging in both the neuronal and the lung cell lines. However, and rather unexpectedly, the ability of the simulants to produce ROS in the surrounding solution was not correlated with the observed cytotoxic or genotoxic effects. We also observed that freshly crushed lunar soil simulants were substantially more effective in causing cell death and DNA damage than were the unprocessed simulants as received from the suppliers.

2. Materials and Methods

2.1. Cell Culture

Proliferating CAD (PCAD) cells were grown in Dulbecco's Modified Eagle's Medium mixed in equal proportion with Ham's F12 medium (DMEM/F12; Hyclone #SH3027201) then supplemented with 10% fetal bovine serum (Corning #MT35010CV) and 1% of a penicillin/streptomycin mixture (Gibco #10378016). Differentiation was stimulated by growing CAD cells in serum-free DMEM/F12, supplemented with 20-μg/ml transferrin and 50 ng/ml sodium selenite. Terminally differentiated CAD (TDCAD) cells were grown on plates coated with poly-L-lysine at 20 mg/ml. Cells were fully differentiated after 5 days (Qi et al., 1997).

A549 cells were grown in Ham's F12 K (Kaighn's) nutrient medium (Gibco #21127022) supplemented with 10% fetal bovine serum and 1% of a penicillin/streptomycin mixture.

2.2. Lunar Soil Simulant Storage and Grinding

Lunar soil simulants were tested in up to three physical states: (i) "as received" from the supplier, (ii) dry-sieved to ≤63 μm using a brass sieve, and (iii) ground to ≤7 μm. These three states were chosen to provide a basis for comparison of the potential toxicity of: (i) as-received materials, (ii) the finest size fraction that can be reliably produced from as-received materials without significant physical processing, and (iii) material that is entirely respirable. The specific surface area of as-received simulants is reported in Kaur et al. (2016) and average ~1 m^2/g. Sieving and grinding can be expected to decrease the average particle size of these materials and increase their specific surface areas.

The ≤7-μm fraction was produced by grinding in a planetary ball mill (Retch PM 100) fitted with an agate grinding container and agate grinding balls at 350 rpm for 10 min. We chose agate grinding media because agate has equivalent or greater hardness than the minerals present in the regolith simulants used and should therefore effectively resist abrasion during the grinding process. The superior performance of agate grinding media was demonstrated by Hickson and Juras (1986) who measured trace element contamination after grinding quartz sand in a variety of grinding containers and showed that agate produced no measurable contamination, even when grinding a phase of equivalent hardness to the grinding media. After grinding, the ≤7-μm samples were placed in vacuum storage in a Labconco vacuum desiccator at ~10-mbar pressure over desiccant. Samples were removed when an aliquot was required for experimentation. One hour before experiments, 0.2 g of the ≤7-μm fraction of each lunar simulant was reground by hand in an agate mortar and pestle for 10 min in order to maximize its reactivity. Based on particle size measurements conducted in our laboratory using a Malvern Mastersizer laser diffraction particle size analyzer, the 10-min regrinding of these <7-μm powders decreased the particle size by <25% in all cases except NU-LHT-2M (decreased 52%). Previous work has shown that long-term storage of powders in vacuum can result in some passivation of their surface reactivity (Hasegawa et al., 1995). We sought to avoid the effects of this surface passivation to place constraints on the maximum possible toxicity of these materials. During hand grinding, lunar simulant accumulated on the sides of the mortar was scraped off regularly to ensure effective grinding of the entire aliquot. Both the mortar and pestle were thoroughly rinsed with water and ethanol before switching samples to prevent contamination between samples.

Table 2
Primers for qPCR

Primer name	Primer sequence (5′-3′)
Mouse mitochondrial long, sense strand	CCATTCTAATCGCCATAGCCTTCC
Mouse mitochondrial long, antisense strand	GAGGACTGGAATGCTGGTTGGTGG
Mouse mitochondrial short, sense strand	CCCAGCTACTACCATCATTCAAGT
Mouse mitochondrial short, antisense strand	GATGGTTTGGGAGATTGGTTGATG
Mouse nuclear (β globin), sense strand	TTGAGACTGTGATTGGCAATGCCT
Mouse nuclear (β globin), antisense strand	CCTTTAATGCCCATCCCGGACT
Human mitochondrial long, sense strand	TCTAAGCCTCCTTATTCGAGCCCGA
Human mitochondrial long, antisense strand	TTTCATCATGCGGAGATGTTGGATGG
Human mitochondrial short, sense strand	CCCCACAAACCCCATTACTAAACCCA
Human mitochondrial short, antisense strand	TTTCATCATGCGGAGATGTTGGATGG

2.3. Trypan Blue Exclusion Dye

Cells were plated in 12-well plates (Corning # 07-200-81) with 1 ml of fully supplemented medium and allowed to grow over night for proliferating cells or 5 days for differentiated cells. Immediately before the experiment, the media in the plates were switched out for 2.5 ml of serum-free media. Lunar soil simulants were measured out into polypropylene tubes then added directly to the medium on the plate with brief gentle mixing. After 1 hr, the media were replaced with fully supplemented media, and the cells were allowed to recover for 24 hr. Cells were released from the plate with 0.5 ml of trypsin-EDTA solution (0.05% trypsin and 0.53 mM ethylenediaminetetraacetic acid; Gemini #400-150) for 10 min, then 80 μl of cell suspension was mixed with 40 μl of 0.4% trypan blue dye (Sigma #T8154). Cells were counted using a hemocytometer under a microscope.

2.4. Quantitative PCR Assay

For dose-response experiments, the 1-hr treatment was as described for the trypan blue exclusion dye experiment. Immediately after the treatment, chromosomal DNA was extracted using the Qiagen 20/G DNA extraction kit (Qiagen #10223) and following the "cell culture" protocol. To avoid removing the mitochondrial DNA from the samples, the cell lysates were not subjected to centrifugation before applying the sample to the DNA isolation columns. The DNA was precipitated with 70% cold ethanol and resuspended in Tris-EDTA by incubation overnight at 4°C. DNA quantification was performed using the Picogreen reagent (Thermo-Fisher P11496).

The PCR assay was based on a previously described protocol (Santos et al., 2002). The primers used are listed in Table 2. Amplification reactions were performed with the mouse mitochondrial primers, for both long and short PCR, in a total volume of 50 μl containing 15 ng DNA template, KAPA Long Range Buffer (KAPA #3503), 100-ng/μl bovine serum albumin, 200 μM each of the four deoxynucleotide triphosphates, 400 nM each of the forward and reverse primers, 1.5-mM $MgCl_2$, and 1 unit of KAPA Long Range Hotstart DNA polymerase (KAPA #3503). The nuclear PCR was identical, with the exception of using 100 μM of each primer. For the short mitochondrial PCR, the thermocycler was programmed for 3 min at 95°C for initial denaturation, followed by 22 cycles of 15 s at 95°C for denaturation, 45 s at 59°C for annealing, 1 min at 68°C for extension, and finished with a final extension at 72°C for 10 min. For the long mitochondrial PCR, the thermocycler was programmed for 3 min at 95°C for initial denaturation, followed by 22 cycles of 15 s at 95°C for denaturation and 12 min at 66°C as annealing and extension, and finished with a final extension at 72°C for 10 min. The long nuclear PCR was programmed for 3 min at 95°C for initial denaturation, followed by 27 cycles of 15 s at 95°C for denaturation and 12 min at 64°C for annealing and extension, and finished with a final extension at 72°C for 10 min.

The long PCR product is 10,965 base pairs, and the short PCR product is 119 base pairs. In order to normalize for this difference, the raw PCR data (which reflect the total mass of material produced) were divided by the product lengths. The control was then normalized to 1.

3. Results

3.1. Cell Survival After Exposure to Lunar Soil Simulants

In order to understand the effect of lunar soil simulants on cell survival, viability was measured in CAD cells exposed to various materials. The cells were challenged with JSC-1A as-received, size sorted to ≤63 μm, or JSC-1A ground to ≤7 μm and reground 1 hr before use. Size sorting or grinding the simulants was

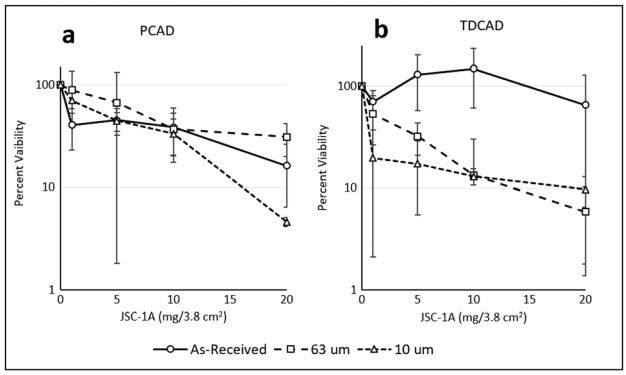

Figure 1. Freshly grinding Johnson Space Center Number One (JSC-1A) may increase its cytotoxicity. Toxicity of JSC-1A, as-received, size-sorted, or ground, on (a) PCAD (proliferating CAD) and (b) TDCAD (terminally differentiated CAD) cells. Cells were treated for 1 hr with JSC-1A as-received, or sieved to ≤63 μm, or ground and sieved to 10 μm, then reground just before use. Cell viability was measured using trypan blue exclusion dye. Results are normalized to untreated cells, which are set to 100%. The error bars indicate the standard deviation (n = 3).

employed for several reasons. Grinding the soil ensures that the average size is small enough that some particles can be engulfed by cells. Because the simulants as-received are naturally varied in size, there may be difficulty in generating consistent responses. Grinding and size sorting produce a more uniform distribution of particle sizes. Crushing the simulants also increases their ability to generate ROS (Hurowitz et al., 2007; Kaur et al., 2016).

A dose-dependent cytotoxic effect was observed for PCAD cells for each of the JSC-1A size classes, with the most significant lethality noted for particles ≤7 μm in size, which reduced cell survival to 10% at 20 mg/3.8 cm^2 (Figure 1a). In the differentiated cells, the ≤63- and ≤7-μm size classes caused similar cytotoxicity, but the as-received JSC-1A did not generate detectable cytotoxicity at doses lower than 20 mg/3.8 cm^2 (Figure 1b). In response to as-received JSC-1A, TDCAD cells showed greater survival than did PCAD cells at every simulant level.

The observed cytotoxicity might be caused by either physical or chemical interaction of the cells with the simulants. To address this question, cells were treated with simulants that were shown to generate ROS with varying effectiveness. CSM-CLF generates ROS in the highest amounts, followed by JSC-1A, with quartz generating the least (Hurowitz et al., 2007; Kaur et al., 2016). Despite these differences, the three materials were similarly cytotoxic to both PCAD (Figure 2a) and TDCAD cells (Figure 2b). The A549 cells were more sensitive than were the CAD cells to both quartz and CSM-CLF (Figure 2c). Conversely, cell killing by JSC-1A was slightly *less* for A549 cells than it was for CAD cells at concentrations less than 15 mg/3.8 cm^2 (Figure 2c).

When the simulants were used in the state received from the suppliers (i.e., not freshly ground), significant CAD cell death was observed only in response to CSM-CLF or anatase (Figure 3a). With freshly ground simulants, 20 mg/3.8 cm^2 of material resulted in high levels of cytotoxicity, but exposure to 10 mg/3.8 cm^2 allowed >10% survival with the majority of these materials. For PCAD and TDCAD cells, fresh grinding increased the cytotoxicity of all the simulants, in some cases slightly more dramatically for TDCAD than for PCAD cells (e.g., both JSC-1A and JSC-1A AGGL; Figure 3b). A549 cells were more sensitive to every simulant than were the

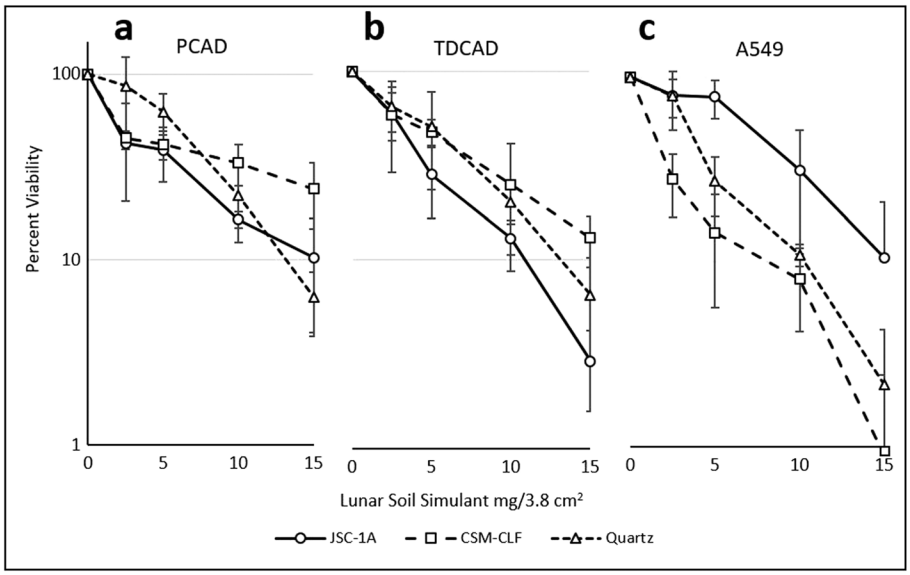

Figure 2. Cytotoxicity is not correlated with reactive oxygen species-generating activity. (a) PCAD (proliferating CAD), (b) TDCAD (terminally differentiated), or (c) A549 cells were treated with increasing concentrations of 10-μm, freshly ground JSC-1A, CSM-CLF, or quartz. Cell viability was assessed using the trypan blue exclusion dye. These results are normalized to untreated cells, which are set to 100%. The error bars are standard deviation (n = 3).

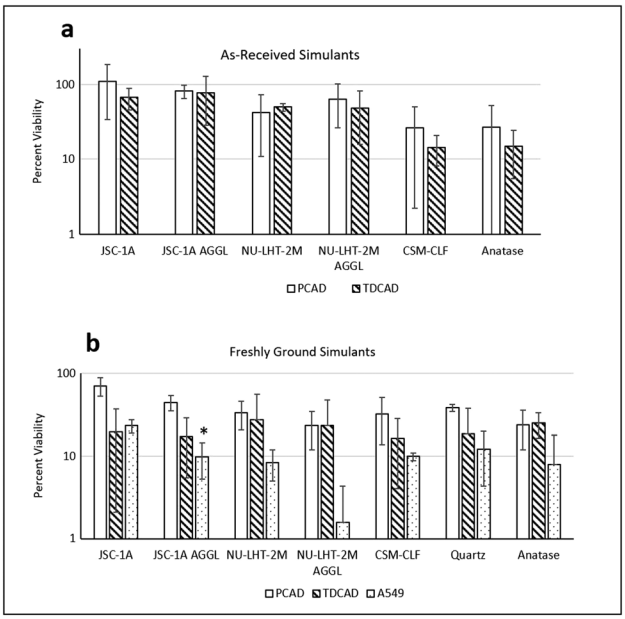

Figure 3. Differential sensitivity of neuronal and lung epithelial cells to various lunar soil simulants. PCAD, proliferating CAD cells; TDCAD, terminally differentiated CAD cells. The cytotoxicity of simulants was compared for (a) 20 mg/3.8 cm^2 as-received material or (b) 10 mg/3.8 cm^2 10-μm material freshly ground 1 hr before use. Cell viability was measured using the trypan blue exclusion dye. The results are normalized to untreated cells, which are set to 100%. The error bars are standard deviation ($n = 3$). * denotes $p < 0.05$ between JSC-1A and JSC-1A AGGL. Quartz was not available when the experiments for (a) were performed.

CAD cells (Figure 3b). Notably, the two agglutinated simulants caused more cell death in the A549 cells did than their unagglutinated counterparts, but such a difference was not seen for CAD cells (Figure 3b).

3.2. DNA Damage From Lunar Soil Simulants

Damage to cellular DNA can lead to mutations, which may be propagated for the life of the organism (Giglia-Mari et al., 2011). The cytotoxic effects of DNA damage can also potentiate cancer by stimulating cell proliferation to replace dead tissue (Labi & Erlacher, 2015). In order to assay the DNA damage resulting from exposure to lunar soil simulants, a PCR-based assay (Furda et al., 2014) was applied to nuclear and mitochondrial DNA isolated from cells after treatment with the simulants. This technique allowed for amplification of the mtDNA specifically, without separately extracting it (Furda et al., 2014). Many DNA template lesions can slow down or block DNA polymerases (Furda et al., 2014; Lehle et al., 2014), so this assay is not specific for the type of damage. However, DNA with fewer lesions is amplified more efficiently than is DNA with greater lesion density, thus giving an indirect measure of the damage.

The ratio of mitochondrial to nuclear DNA can vary as a result of the isolation procedure, the cell treatment, or cell-type differences. Thus, a separate set of PCR reactions was performed to amplify a small (~100-base-pair) region of either mtDNA or a single-copy nuclear gene, and the resulting values were used to normalize the respective long PCR values that are sensitive to the presence of DNA lesions. The short segments used for this normalization are unlikely to contain a lesion at biologically relevant levels of DNA damage (Furda et al., 2014; Lehle et al., 2014).

PCAD cells and TDCAD cells showed strikingly different levels of DNA damage after simulant exposure (Figure 4). The PCAD cells had little detectable damage in their nuclear DNA after exposure to any of the freshly ground simulants at 10 mg/3.8 cm^2, while the DNA damage detected in TDCAD cells was very high for all the simulants (Figure 4a). The DNA damage caused by quartz and anatase was measured at 5 mg/3.8 cm^2, because greater amounts of those materials gave levels of DNA damage too high to permit a measurement. The TDCAD cells suffered modest but significant nuclear DNA damage after quartz or anatase treatment, while little or no DNA damage was detected in PCAD cells (Figure 4b). Similarly to the freshly ground simulants, the as-received simulants caused greater nuclear DNA damage to the TDCAD than to the PCAD cells, with no detectable damage in the PCAD nuclear DNA (Figure 4c). The DNA damage results contrast with the cell viability data, which showed similar survival outcomes for PCAD and TDCAD cells for most of the simulants (Figure 1). We were not able to measure nuclear DNA damage in A549 cells because not enough DNA could be extracted from A549 cells to measure both nuclear and mitochondrial DNA damage (Furda et al., 2014).

The results for mtDNA damage were mostly reversed from those observed for nuclear DNA. Exposure to most of the freshly ground simulants generated less detectable mtDNA damage (i.e., greater amounts of PCR product) in the TDCAD than in the PCAD cells (Figure 5a). The converse was seen for cells exposed to quartz or anatase (Figure 5b). Of the unground simulants, only CSM-CLF caused significant mtDNA damage in CAD cells, at about equal levels for PCAD and TDCAD (Figure 5c). The A549 cells suffered only moderate levels of mtDNA damage after exposure to any of the freshly ground simulants (Figure 5a).

4. Discussion

We found that exposure of neuronal and lung epithelial cells in culture to several types of lunar soil simulants caused cell death and DNA damage. The effects varied with the cell type, including whether the CAD cells were in the proliferating (precursor) or the fully differentiated (neuronal) state. In general, using material

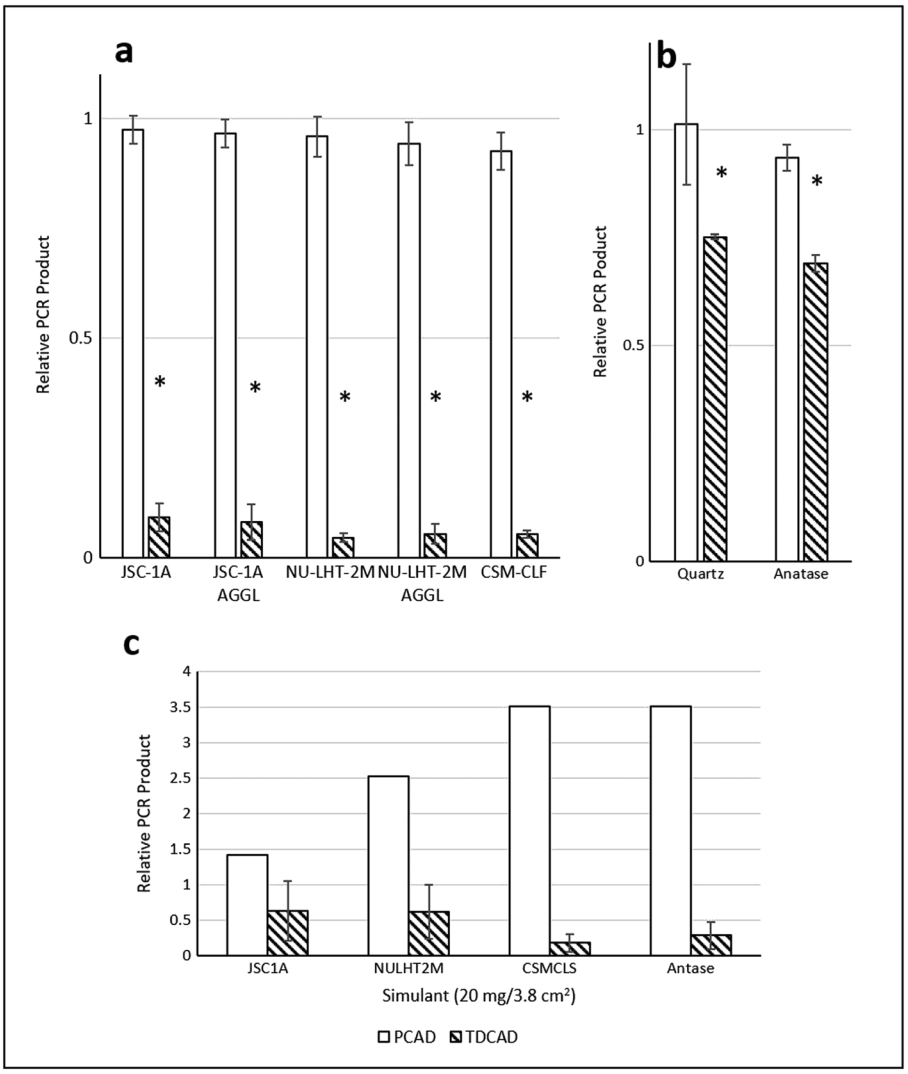

Figure 4. Greater nuclear DNA damage in TDCAD (terminally differentiated CAD) than in PCAD (proliferating CAD) cells exposed to freshly ground or as-received lunar soil simulants. Cells were treated with the indicated simulant for 1 hr, then total DNA was immediately extracted for PCR. (a) The 10 mg/3.8 cm^2 freshly ground simulant or (b) 5 mg/3.8 cm^2 freshly ground simulant. (c) Cells treated with 20 mg/3.8 cm^2 lunar soil simulants as-received. PCAD cells treated with as-received simulants have $n = 2$ due to a lack of DNA extracted from the cells. Results are normalized to untreated cells, which are set to 1. The error bars indicate standard deviation ($n = 3$). * denotes $p < 0.05$ between PCAD and TDCAD treatments.

that had been freshly ground produced much greater effects than were seen with the simulants as received from the supplier. At first glance, our results would thus seem in line with the prior observations on ROS production (Hurowitz et al., 2007; Kaur et al., 2016). However, there was no consistent variation of either the cytotoxicity or the DNA-damaging capacity of the materials with their ability to generate ROS in solution. Thus, the cellular (and likely, the tissue-level) effects of these particulate, regolith-simulating materials are more complex than simply the ability to generate measurable ROS in the medium.

The grinding procedure has at least two effects that could increase the biological impact of the lunar soil simulants. The increase in surface area per unit volume would certainly increase the availability of reactive components, such as iron, to participate in ROS-generating reactions. Perhaps more importantly, the smaller sizes of the particles resulting from grinding would bring them into the range of microscopic interaction with the cells, which could even enable cellular uptake of the smallest particles (Champion et al., 2008). It is worth noting in this context that ROS generated by internalized (phagocytosed) particles would likely be undetectable in the surrounding solution. Uptake of even chemically inert particles also stimulates active ROS production in a wide range of cell types via an inflammatory response (Champion et al., 2008; Gustafson et al., 2015).

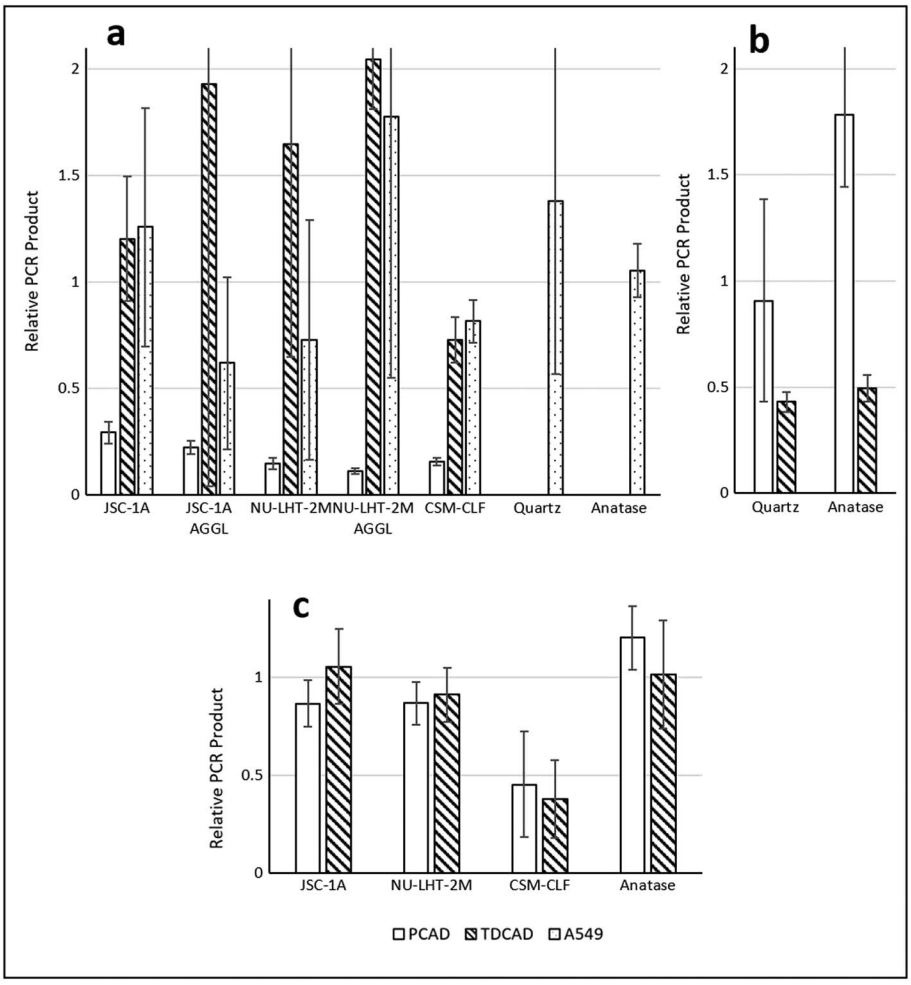

Figure 5. PCAD (proliferating CAD) cells may undergo more mtDNA damage than do TDCAD (terminally differentiated CAD) or A549 cells. Cells were treated with the indicated simulant for 1 hr, followed by immediate DNA was extraction for PCR. (a) Cells treated with 10 mg/3.8 cm^2 freshly ground lunar soil simulants. (b) Cells treated with 5 mg/cm^2 freshly ground quartz and anatase. (c) Cells treated with 20 mg/3.8 cm^2 lunar soil simulants as-received. Results are normalized to untreated cells, which are set to 1. The error bars indicate standard deviation (n = 3).

In this context, we note that as-received anatase exerted as much cytotoxicity in CAD cells as did CSM-CLF, despite the significant difference in chemical reactivity between these materials. This result is, however, consistent with dominance in cell killing of nonchemical effects of the particles, such as the activation of inflammatory responses.

Conversely, the impact of externally generated ROS would be greatly dampened by cellular antioxidant enzymes such as catalase, glutathione peroxidase, superoxide dismutase, and by small molecules such as glutathione (Oyewole & Birch-Machin, 2015). The potential impact of lunar regolith on human tissues and the resulting health effects of the particles will thus have to be assessed in light of their ability to be engulfed by cells or transmitted to deeper tissues, as occurs with particle uptake into the brains of mice following nasal inhalation (Hopkins et al., 2014). In addition, the results indicate that the ability of the particles to generate ROS *within* cells should be investigated, as this capacity might differ significantly from what is measured with the materials alone in solution (Fu et al., 2014).

The cell-type differences in the effects of the various simulants merit some comment. The similar cell-killing ability of the freshly ground materials for PCAD and TDCAD cells was unexpected, as cycling cells are typically more sensitive to DNA-damaging agents than are nonreplicating cells. This typical pattern results from the vulnerability of cellular DNA to damage during replication and from the need for an undamaged DNA template for efficient DNA synthesis (Iyama & Wilson, 2013). The similar responses to simulant exposure of

PCAD and TDCAD cells is thus a further indication that damage to DNA is not necessarily a critical component of the cytotoxicity.

The A549 lung epithelial cells appeared to be less sensitive to killing by freshly ground JSC-1A than were either PCAD or TDCAD cells. Whether this difference indicates greater protective mechanisms in lung epithelial cells than in neurons will require additional study. However, the observation suggests that the extended projections of TDCAD cells (Qi et al., 1997), like the axons and dendrites in neuronal tissues, do not necessarily render them more susceptible to lethal damage to cellular membranes, proteins, mitochondria, or other vital organelles.

It is noteworthy that mtDNA damage was not well correlated with cell survival. The apparent lack of mtDNA damage in the simulant-treated TDCAD cells could arise in two ways. The capacity of mtDNA repair could be greater in the differentiated than in the proliferating CAD cells, but we have not observed such a difference for chemical DNA-damaging agents. It is also possible that damaged mtDNA is eliminated rapidly in TDCAD cells, within the 1-hr treatment period we used, such that none is detected in the assay. Elimination of heavily damaged mtDNA has been observed in other cases (Kandul et al., 2016; Moretton et al., 2017) and is an effective option for mitochondria owing to the presence of multiple copies of mtDNA within a single compartment in the cell.

Clearly, avoidance of lunar dust inhalation will be important for future explorers, but with increased human activity on the Moon it is likely that adventitious exposure will occur, particularly for individuals spending long periods of time on that body. A detailed understanding of the health effects of lunar dust exposure is thus important, and further defining the cellular and biological impact of materials from various parts of the lunar surface is warranted. It will be critical to study actual lunar regolith samples for their effects on cell function and the integrity of the cellular DNA.

Acknowledgments
We thank Martin Schoonen and Jasmeet Kaur for advice and assistance with some of the initial experiments. We thank the S. Tsirka lab and our colleagues in the Demple lab for helpful discussions. The underlying data for this article will be deposited in Stony Brook University's Academic Commons data repository http://commons.library.stonybrook.edu/geo-articles/, where they will be publicly available. This work was supported by a grant from NASA (NNA-14AB04A; T. Glotch, Stony Brook University, PI).

References

Baxter, P. J., Ing, R., Falk, H., & Plikaytis, B. (1983). Mount St. Helens eruptions: The acute respiratory effects of volcanic ash in a North American community. *Archives of Environmental Health*, *38*(3), 138–143.

Bhagia, L. J. (2012). Non-occupational exposure to silica dust. *IndianJournal of Occupational and Environmental Medicine*, *16*(3), 95–100. https://doi.org/10.4103/0019-5278.111744

Campbell, A., Oldham, M., Becaria, A., Bondy, S. C., Meacher, D., Sioutas, C., et al. (2005). Particulate matter in polluted air may increase biomarkers of inflammation in mouse brain. *Neurotoxicology*, *26*(1), 133–140. https://doi.org/10.1016/j.neuro.2004.08.003

Cha, M. Y., Kim, D. K., & Mook-Jung, I. (2015). The role of mitochondrial DNA mutation on neurodegenerative diseases. *Experimental & Molecular Medicine*, *47*, e150. https://doi.org/10.1038/emm.2014.122

Champion, J. A., Walker, A., & Mitragotri, S. (2008). Role of particle size in phagocytosis of polymeric microspheres. *Pharmaceutical Research*, *25*(8), 1815–1821. https://doi.org/10.1007/s11095-008-9562-y

Colwell, J. E., Batiste, S., Horányi, M., Robertson, S., & Sture, S. (2007). Lunar surface: Dust dynamics and regolith mechanics. *Reviews of Geophysics*, *45*, RG2006. https://doi.org/10.1029/2005rg000184

Fu, P. P., Xia, Q., Hwang, H. M., Ray, P. C., & Yu, H. (2014). Mechanisms of nanotoxicity: generation of reactive oxygen species. *Journal of Food and Drug Analysis*, *22*(1), 64–75. https://doi.org/10.1016/j.jfda.2014.01.005

Furda, A., Santos, J. H., Meyer, J. N., & Van Houten, B. (2014). Quantitative PCR-based measurement of nuclear and mitochondrial DNA damage and repair in mammalian cells. *Methods in Molecular Biology*, *1105*, 419–437. https://doi.org/10.1007/978-1-62703-739-6_31

Gaier, J. R. (2007). The effects of lunar dust on EVA systems during the Apollo missions.

Giglia-Mari, G., Zotter, A., & Vermeulen, W. (2011). DNA damage response. *Cold Spring Harbor Perspectives in Biology*, *3*(1), a000745. https://doi.org/10.1101/cshperspect.a000745

Gustafson, H. H., Holt-Casper, D., Grainger, D. W., & Ghandehari, H. (2015). Nanoparticle uptake: The phagocyte problem. *Nano Today*, *10*(4), 487–510. https://doi.org/10.1016/j.nantod.2015.06.006

Hasegawa, M., Ogata, T., & Sato, M. (1995). Mechano-radicals produced from ground quartz and quartz glass. *Powder Technology*, *85*(3), 269–274. https://doi.org/10.1016/0032-5910(96)80150-1

Heiken, G., Vaniman, D., & French, B. M. (1992). Lunar sourcebook. A user's guide to the Moon. *Endeavour*, *16*(2), 1–736.

Hickson, C. J., & Juras, S. J. (1986). Sample contamination by grinding. *Canadian Mineralogist*, *24*, 585–589.

Hopkins, L. E., Patchin, E. S., Chiu, P. L., Brandenberger, C., Smiley-Jewell, S., & Pinkerton, K. E. (2014). Nose-to-brain transport of aerosolised quantum dots following acute exposure. *Nanotoxicology*, *8*(8), 885–893. https://doi.org/10.3109/17435390.2013.842267

Hurowitz, J. A., Tosca, N. J., McLennan, S. M., & Schoonen, M. A. A. (2007). Production of hydrogen peroxide in Martian and lunar soils. *Earth and Planetary Science Letters*, *255*(1–2), 41–52. https://doi.org/10.1016/j.epsl.2006.12.004

Iyama, T., & Wilson, D. M. 3rd. (2013). DNA repair mechanisms in dividing and non-dividing cells. *DNA Repair (Amst)*, *12*(8), 620–636. https://doi.org/10.1016/j.dnarep.2013.04.015

Jabbal, S., Poli, G., & Lipworth, B. (2017). Does size really matter?: Relationship of particle size to lung deposition and exhaled fraction. *The Journal of Allergy and Clinical Immunology*, *139*(6), 2013–2014.e1. https://doi.org/10.1016/j.jaci.2016.11.036

Kandul, N. P., Zhang, T., Hay, B. A., & Guo, M. (2016). Selective removal of deletion-bearing mitochondrial DNA in heteroplasmic Drosophila. *Nature Communications*, *7*, 13100. https://doi.org/10.1038/ncomms13100

Kaur, J., Rickman, D., & Schoonen, M. A. (2016). Reactive oxygen species (ROS) generation by lunar simulants. *Acta Astronautica*, *122*, 196–208. https://doi.org/10.1016/j.actaastro.2016.02.002

Labi, V., & Erlacher, M. (2015). How cell death shapes cancer. *Cell Death & Disease*, *6*, e1675. https://doi.org/10.1038/cddis.2015.20
Lam, C. W., James, J. T., McCluskey, R., Cowper, S., Balis, J., & Muro-Cacho, C. (2002). Pulmonary toxicity of simulated lunar and Martian dusts in mice: I. Histopathology 7 and 90 days after intratracheal instillation. *Inhalation Toxicology*, *14*(9), 901–916. https://doi.org/10.1080/08958370290084683
Lam, C. W., Scully, R. R., Zhang, Y., Renne, R. A., Hunter, R. L., McCluskey, R. A., et al. (2013). Toxicity of lunar dust assessed in inhalation-exposed rats. *Inhalation Toxicology*, *25*(12), 661–678. https://doi.org/10.3109/08958378.2013.833660
Lehle, S., Hildebrand, D. G., Merz, B., Malak, P. N., Becker, M. S., Schmezer, P., et al. (2014). LORD-Q: A long-run real-time PCR-based DNA-damage quantification method for nuclear and mitochondrial genome analysis. *Nucleic Acids Research*, *42*(6), e41. https://doi.org/10.1093/nar/gkt1349
Mckay, D. S., Cooper, B. L., Taylor, L. A., James, J. T., Thomas-Keprta, K., Pieters, C. M., et al. (2015). Physicochemical properties of respirable-size lunar dust. *Acta Astronautica*, *107*, 163–176. https://doi.org/10.1016/j.actaastro.2014.10.032
Moretton, A., Morel, F., Macao, B., Lachaume, P., Ishak, L., Lefebvre, M., et al. (2017). Selective mitochondrial DNA degradation following double-strand breaks. *PLoS One*, *12*(4), e0176795. https://doi.org/10.1371/journal.pone.0176795
Oberdörster, G., Oberdörster, E., & Oberdörster, J. (2005). Nanotoxicology: An emerging discipline evolving from studies of ultrafine particles. *Environmental Health Perspectives*, *113*(7), 823–839. https://doi.org/10.1289/ehp.7339
Oberdörster, G., Sharp, Z., Atudorei, V., Elder, A., Gelein, R., Kreyling, W., & Cox, C. (2004). Translocation of inhaled ultrafine particles to the brain. *Inhalation Toxicology*, *16*(6–7), 437–445. https://doi.org/10.1080/08958370490439597
Oyewole, A. O., & Birch-Machin, M. A. (2015). Mitochondria-targeted antioxidants. *The FASEB Journal*, *29*(12), 4766–4771. https://doi.org/10.1096/fj.15-275404
Qi, Y. P., Wang, J. K. T., McMillian, M., & Chikaraishi, D. M. (1997). Characterization of a CNS cell line, CAD, in which morphological differentiation is initiated by serum deprivation. *Journal of Neuroscience*, *17*(4), 1217–1225.
Ray, C. S., Reis, S. T., Sen, S., & O'Dell, J. S. (2010). JSC-1A lunar soil simulant: Characterization, glass formation, and selected glass properties. *Journal of Non-Crystalline Solids*, *356*(44–49), 2369–2374. https://doi.org/10.1016/j.jnoncrysol.2010.04.049
Rimal, B., Greenberg, A. K., & Rom, W. N. (2005). Basic pathogenetic mechanisms in silicosis: Current understanding. *Current Opinion in Pulmonary Medicine*, *11*(2), 169–173.
Roos, W. P., & Kaina, B. (2013). DNA damage-induced cell death: from specific DNA lesions to the DNA damage response and apoptosis. *Cancer Letters*, *332*(2), 237–248. https://doi.org/10.1016/j.canlet.2012.01.007
Roos, W. P., Thomas, A. D., & Kaina, B. (2016). DNA damage and the balance between survival and death in cancer biology. *Nature Reviews. Cancer*, *16*(1), 20–33. https://doi.org/10.1038/nrc.2015.2
Santos, J. H., Mandavilli, B. S., & Van Houten, B. (2002). Measuring oxidative mtDNA damage and repair using quantitative PCR. *Methods in Molecular Biology*, *197*, 159–176. https://doi.org/10.1385/1-59259-284-8:159
Sena, L. A., & Chandel, N. S. (2012). Physiological roles of mitochondrial reactive oxygen species. *Molecular Cell*, *48*(2), 158–167. https://doi.org/10.1016/j.molcel.2012.09.025
Stubbs, T. J., Vondrak, R. R., & Farrell, W. M. (2005). A dynamic fountain model for lunar dust. *Advances in Space Research*, *37*(1), 59–66.
Turci, F., Corazzari, I., Alberto, G., Martra, G., & Fubini, B. (2015). Free-radical chemistry as a means to evaluate lunar dust health hazard in view of future missions to the Moon. *Astrobiology*, *15*(5), 371–380. https://doi.org/10.1089/ast.2014.1216
Upadhyay, D., Panduri, V., Ghio, A., & Kamp, D. W. (2003). Particulate matter induces alveolar epithelial cell DNA damage and apoptosis: Role of free radicals and the mitochondria. *American Journal of Respiratory Cell and Molecular Biology*, *29*(2), 180–187. https://doi.org/10.1165/rcmb.2002-0269OC
van Berlo, D., Wessels, A., Boots, A. W., Wilhelmi, V., Scherbart, A. M., Gerloff, K., et al. (2010). Neutrophil-derived ROS contribute to oxidative DNA damage induction by quartz particles. *Free Radical Biology & Medicine*, *49*(11), 1685–1693. https://doi.org/10.1016/j.freeradbiomed.2010.08.031
Wagner, S. A. (2006). The Apollo experience lessons learned for constellation lunar dust management *lunar and planetary science and exploration* (58 pp.). ntrs.nasa.gov: NASA.
Wang, Y., Sun, H., Tan, S., Feng, H., Cheng, Z., Zhao, J., et al. (2013). Role of point defects on the reactivity of reconstructed anatase titanium dioxide (001) surface. *Nature Communications*, *4*, 2214. https://doi.org/10.1038/ncomms3214
Warheit, D. B., Webb, T. R., Reed, K. L., Frerichs, S., & Sayes, C. M. (2007). Pulmonary toxicity study in rats with three forms of ultrafine-TiO_2 particles: Differential responses related to surface properties. *Toxicology*, *230*(1), 90–104. https://doi.org/10.1016/j.tox.2006.11.002
Yauk, C., Polyzos, A., Rowan-Carroll, A., Somers, C. M., Godschalk, R. W., Van Schooten, F. J., et al. (2008). Germ-line mutations, DNA damage, and global hypermethylation in mice exposed to particulate air pollution in an urban/industrial location. *Proceedings of the National Academy of Sciences of the United States of America*, *105*(2), 605–610. https://doi.org/10.1073/pnas.0705896105